Research Square

Preprints are preliminary reports that have not undergone peer review.
They should not be considered conclusive, used to inform clinical practice,
or referenced by the media as validated information.

Cumulative-Sensing-Aware Fixed-Point Iterationfor Spatial-Reuse Estimation in Two-DimensionalCSMA/CA Ad-Hoc Networks

Anh Tuan GIANG

giang-anh.tuan@usth.edu.vn

University of Science and Technology of Hanoi

Nhat Quang DOAN

University of Science and Technology of Hanoi

Hoang Ha NGUYEN

University of Science and Technology of Hanoi

Thai Luan VU

Texas Tech University

Research Article

Keywords: CSMA/CA, spatial reuse, fixed-point iteration, cumulative sensing, ad-hoc networks, Wi-Fi, carrier-sense threshold

Posted Date: June 2nd, 2026

DOI: https://doi.org/10.21203/rs.3.rs-9807297/v1

License: This work is licensed under a Creative Commons Attribution 4.0 International License.
Read Full License

Additional Declarations: No competing interests reported.

Cumulative-Sensing-Aware Fixed-Point Iteration for Spatial-Reuse Estimation in Two-Dimensional CSMA/CA Ad-Hoc Networks

Anh Tuan GIANG[1*], Nhat Quang DOAN[1],
Hoang Ha NGUYEN[1], Thai Luan VU[2]

[1]University of Science and Technology of Hanoi, Vietnam Academy of Science and Technology, 18 Hoang Quoc Viet, Nghia Do ward, Hanoi, Vietnam.
[2]Department of Mathematics and Statistics, Texas Tech University, 2500 Broadway, Lubbock, Texas, United States.

*Corresponding author(s). E-mail(s): giang-anh.tuan@usth.edu.vn;
Contributing authors: doan-nhat.quang@usth.edu.vn;
nguyen-hoang.ha@usth.edu.vn; vu.luan@ttu.edu;

Abstract

How many transmitters can speak at the same time in a CSMA/CA wireless network? Although this question lies at the heart of spatial reuse, it remains difficult to answer in finite two-dimensional deployments where carrier sensing is governed by aggregate received energy rather than simple pairwise distances. This paper introduces a cumulative-sensing-aware fixed-point formulation for estimating the expected number of simultaneous transmitters in two-dimensional CSMA/CA ad-hoc networks. The network region is discretized into candidate transmitter locations, and each state is defined by the subset of currently active transmitters. For every state, a candidate transmitter is feasible only if the cumulative sensing energy generated by all active transmitters does not exceed the CCA threshold. This leads to a finite-state fixed-point equation whose solution gives the expected spatial-reuse factor, measured as the mean number of simultaneously active transmitters. The proposed estimator is deterministic, physically interpretable, and directly parameterized by transmit power, reference path loss, path-loss exponent, and CCA threshold. We validate the model against ns-3.46.1 ad-hoc Wi-Fi simulations under variations in area size, node count, path-loss exponent, and CCA threshold. The fixed-point estimates closely match ns-3

results across 101 validation cases, with an average relative error of approximately 2.41%. These results demonstrate that cumulative carrier sensing is a dominant geometric mechanism behind CSMA/CA spatial reuse and that the proposed fixed-point framework accurately estimates the concurrency component of spatial-reuse factor.

Keywords: CSMA/CA, spatial reuse, fixed-point iteration, cumulative sensing, ad-hoc networks, Wi-Fi, carrier-sense threshold

1 Introduction

Spatial reuse is one of the fundamental mechanisms that allows wireless networks to scale. In a CSMA/CA network, the same channel can be reused by multiple transmitters when they are sufficiently separated in space. This simple idea is central to the performance of Wi-Fi ad-hoc networks, dense WLANs, mesh networks, vehicular networks, and many emerging distributed wireless systems. However, estimating how many transmitters can be active at the same time remains a nontrivial problem, especially when the network is deployed in a finite two-dimensional region and carrier sensing depends on the cumulative energy produced by all ongoing transmissions.

Classical analyses of CSMA/CA and IEEE 802.11 networks have provided important insights into contention, backoff, and throughput performance. Many analytical models, however, either focus on MAC-layer contention probabilities, assume one-dimensional topologies, or simplify spatial reuse through pairwise exclusion regions. In such models, a candidate transmitter is often blocked if it is too close to an active transmitter. While this pairwise view is mathematically convenient, it does not fully reflect the physical carrier-sensing mechanism used in practical Wi-Fi systems. In reality, a station senses the aggregate received energy over the channel. Therefore, even if no single active transmitter is strong enough to block a candidate station, the sum of several weaker signals may still exceed the CCA threshold and prevent transmission. This cumulative-sensing effect is especially important in two-dimensional deployments, where multiple active transmitters may surround a candidate node from different directions.

Packet-level network simulators such as ns-3 can model these effects with high fidelity. They include PHY-layer propagation, MAC contention, random backoff, transmission timing, and configurable CCA thresholds. However, simulation-based evaluation is computationally expensive when one needs to explore a large parameter space involving area size, node density, path-loss exponent, transmit power, and carrier-sensing threshold. Moreover, simulation alone does not directly provide a compact mathematical explanation of how geometry and cumulative sensing jointly determine spatial reuse. This motivates the need for an analytical or numerical estimator that is simple enough to be interpretable, but accurate enough to match packet-level simulation.

In this paper, we propose a cumulative-sensing-aware fixed-point formulation for estimating the expected number of simultaneous transmitters in a two-dimensional

CSMA/CA ad-hoc network. The deployment area is discretized into a finite set of candidate transmitter locations. For every possible active-transmitter set, the model computes the cumulative received sensing energy at each inactive candidate location. A candidate is considered feasible only if this aggregate energy does not exceed the CCA threshold. Starting from the empty active set, the proposed method estimates the expected number of transmitters that can be sequentially admitted before no further candidate remains feasible.

The key idea is to view spatial reuse as a finite-state admission process. Each state corresponds to a subset of currently active transmitters. From a given state, the feasible action set contains all candidate transmitters that can still access the channel under the cumulative carrier-sensing constraint. The expected number of additional admissible transmitters satisfies a fixed-point equation over this state space. Unlike pairwise carrier-sensing models, the proposed formulation explicitly accounts for the aggregate energy generated by the entire active set. As a result, it captures the fact that spatial reuse is not determined only by pairwise distances, but by the global geometric configuration of simultaneous transmitters.

The proposed fixed-point estimator is deterministic. It does not rely on Monte Carlo sampling and therefore produces reproducible estimates for a given geometry and physical configuration. At the same time, it remains closely connected to practical Wi-Fi parameters. The propagation model uses a capped log-distance path-loss function consistent with the ns-3 validation setup. The transmit power, reference loss, path-loss exponent, and CCA threshold are directly parameterized in physical units. This makes the model suitable not only for theoretical reasoning, but also for comparison with packet-level simulation.

We validate the proposed estimator using ns-3.46.1 simulations of an ad-hoc Wi-Fi UDP broadcast network. The validation considers four complementary scenarios: increasing deployment area with a fixed number of candidate transmitters, increasing node count in a fixed area, varying the path-loss exponent, and varying the CCA threshold. Across these scenarios, the fixed-point estimates closely follow the ns-3 results, including the saturation behavior under dense deployments, the increase in spatial reuse under stronger path loss, and the reduction in simultaneous transmissions under more sensitive CCA thresholds. Over all validation cases, the estimator achieves a small average relative error, showing that cumulative carrier sensing is the dominant mechanism governing the observed spatial-reuse factor.

The main contributions of this paper are summarized as follows:

- We formulate the spatial-reuse factor estimation problem for two-dimensional CSMA/CA ad-hoc networks under cumulative carrier sensing.
- We derive a finite-state fixed-point equation that estimates the expected number of simultaneous transmitters by recursively evaluating feasible transmitter admissions.
- We implement an exact deterministic solver based on grid-center candidate placement, pairwise gain precomputation, and cumulative sensing-energy evaluation over active-transmitter subsets.
- We validate the proposed estimator against ns-3.46.1 ad-hoc Wi-Fi simulations across deployment area, node count, path-loss exponent, and CCA-threshold variations.

- We show that the proposed method provides an interpretable and accurate alternative to exhaustive packet-level simulation for estimating spatial-reuse factor in finite two-dimensional CSMA/CA networks.

The remainder of this paper is organized as follows. Section 2 reviews related work on CSMA/CA modeling, spatial reuse, and analytical capacity estimation. Section 3 introduces the two-dimensional network model and cumulative carrier-sensing formulation. Section 4 presents the fixed-point equation and the deterministic solution procedure. Section 5 describes the ns-3 validation setup and discusses the simulation results. Finally, Section 7 concludes the paper and outlines future research directions.

2 Related Work

Analytical modeling of CSMA/CA networks has a long and influential history. A natural starting point is the seminal IEEE 802.11 Distributed Coordination Function (DCF) model of Bianchi, which introduced a two-dimensional Markov-chain analysis for saturation throughput under idealized single-cell assumptions [1]. This work established the value of compact stochastic abstractions for random-access MAC protocols and remains the baseline for much of the WLAN modeling literature. Subsequent studies extended this foundation to incorporate non-saturation, heterogeneous traffic, PHY-layer effects, and newer IEEE 802.11 amendments. Malone *et al.* considered nonsaturated heterogeneous conditions [2], while other works developed refined Markov-chain or protocol-specific models for IEEE 802.11, IEEE 802.11g, and IEEE 802.11n networks [3–6]. These studies improve protocol realism, but they generally remain centered on MAC-layer contention and throughput, while the spatial interaction among simultaneously active transmitters is either simplified or indirectly represented.

A second important line of work moved from explicit Markov-chain enumeration to fixed-point formulations. Kumar *et al.* showed that single-cell IEEE 802.11 WLAN behavior can be characterized through fixed-point relations among node attempt processes, providing new insight into the decoupling approximation [7]. This fixed-point viewpoint is particularly relevant to the present paper because it demonstrates that complicated MAC interactions can be represented by deterministic self-consistency equations. However, most classical fixed-point WLAN models focus on attempt probabilities, service rates, or throughput in single-cell or effectively homogeneous settings. In contrast, the present work uses a fixed-point equation to estimate a spatial-reuse factor in a finite two-dimensional geometry, where the feasible active-transmitter set depends on cumulative carrier sensing.

Multi-hop CSMA networks introduce additional spatial effects such as partial carrier sensing, starvation, and unfairness. Liew *et al.* developed a back-of-the-envelope approach for computing throughput distributions in CSMA wireless networks using an ideal-CSMA viewpoint [8]. Garetto *et al.* studied per-flow throughput and starvation in CSMA multi-hop wireless networks, showing that spatial topology can strongly affect fairness and performance [9]. Durvy *et al.* analyzed self-organization properties of CSMA/CA systems and their consequences on fairness [10], while Jiang and Walrand connected CSMA operation to distributed scheduling, throughput, and utility

maximization [11]. Laufer and Kleinrock further characterized the capacity region of wireless CSMA/CA networks under arbitrary topologies and unsaturated traffic [12]. These works show that CSMA/CA performance is fundamentally shaped by the set of links or nodes that can be active together. Nevertheless, many of them represent spatial compatibility through pairwise conflict graphs or contention relations, rather than through aggregate sensed energy from all active transmitters.

Carrier-sensing models based on pairwise exclusion are analytically convenient, but they may be insufficient when multiple weak transmitters jointly raise the sensed energy above the CCA threshold. This issue was directly addressed by Fu *et al.*, who studied effective carrier sensing in CSMA networks under cumulative interference and showed that safe carrier-sensing design under aggregate interference differs significantly from pairwise reasoning [13]. Chau *et al.* further investigated static and adaptive carrier sensing for dense wireless CSMA networks, including cumulative-interference-power and incremental-interference-power carrier-sensing mechanisms [14]. Threshold-based spatial reuse has also been examined in high-density CSMA/CA MIMO networks, where the physical carrier-sense threshold controls the tradeoff between concurrency and interference [15]. These studies are among the closest to the present work because they explicitly recognize the importance of aggregate sensing or threshold adaptation. However, they are mainly concerned with safe carrier-sense design, goodput, fairness, or dense-network threshold selection, whereas our objective is to construct a deterministic finite-state estimator for the expected number of simultaneous transmitters in a bounded two-dimensional deployment.

A parallel body of work models CSMA networks through stochastic geometry and hard-core point processes. In this view, the active transmitter set is approximated by a repulsive spatial point process, often derived from Matérn-type thinning of an underlying Poisson point process. ElSawy and Hossain proposed a modified hard-core point process for random CSMA wireless networks under fading, improving the estimation of active-transmitter density compared with simpler hard-core approximations [16]. Alfano *et al.* developed stochastic-geometry tools for dense CSMA networks, including throughput distributions and non-Poisson placements [17]. Sun *et al.* also modeled and analyzed random dense CSMA networks, emphasizing that classical hard-core models may under- or over-estimate concurrent-transmitter density depending on how freezing behavior and fading are represented [18]. These stochastic-geometry models are valuable because they capture spatial randomness and spatial exclusion in large networks. However, their outputs are usually spatial averages, active-transmitter densities, or distributional quantities over random deployments. The present paper instead targets a deterministic estimate for a concrete finite geometry, which is useful when the node layout and physical parameters are explicitly known.

Related analytical techniques also appear in IEEE 802.15.4, wireless sensor networks, and IoT MAC modeling. Ramachandran *et al.* analyzed the contention access period of the IEEE 802.15.4 MAC [19], while Alves and Margi used Colored Petri Nets to model IEEE 802.15.4 beacon-enabled operation [20]. More recently, Ortín *et al.* modeled the coexistence of ALOHA-based PCA and CSMA/CA in unslotted IEEE 802.15.4 networks [21]. These works reinforce the broader point that finite-state abstractions can be effective for random-access MAC analysis. However, their main

focus is low-power IoT or sensor-network operation, not dense WLAN-style spatial reuse under cumulative carrier sensing.

Vehicular ad-hoc networks provide another relevant context because spatial reuse, topology, and carrier sensing directly affect broadcast performance and safety-message dissemination. Ghandour *et al.* studied IEEE 802.11p/WAVE safety-message dissemination and proposed analytical and protocol-level enhancements [22]. Giang *et al.* investigated topology control and capacity estimation in VANETs [23], then developed models and optimization methods for CSMA/CA in vehicular ad-hoc networks [24]. A subsequent study analyzed the spatial capacity of IEEE 802.11p-based VANETs using models, simulations, and experiments [25]. These vehicular works are especially relevant because they treat simultaneous transmissions and spatial capacity as first-order performance quantities. The present paper extends this line of thinking beyond one-dimensional road-like or vehicular settings toward a more general finite two-dimensional CSMA/CA deployment with cumulative sensing.

Recent IEEE 802.11ax research has renewed interest in spatial reuse through mechanisms such as BSS coloring and OBSS/PD-based carrier-sense adaptation. Khorov *et al.* provided a detailed tutorial on IEEE 802.11ax high-efficiency WLANs, including mechanisms designed to improve dense-network operation and spatial reuse [26]. Wilhelmi *et al.* studied spatial reuse in IEEE 802.11ax WLANs using analytical and simulation-based tools [27]. Lanante and Roy analyzed OBSS_PD-based spatial reuse and showed how threshold-based mechanisms can improve concurrent transmissions and area throughput under suitable conditions [28]. Although these works are mainly infrastructure-oriented rather than ad-hoc, they confirm the importance of carrier-sense thresholds in regulating spatial reuse. Our work is complementary: instead of analyzing a standards-specific OBSS/PD mechanism, we focus on a generic cumulative-sensing model for estimating the expected number of simultaneous transmitters in finite two-dimensional ad-hoc networks.

Overall, existing studies provide powerful tools for IEEE 802.11 DCF analysis, fixed-point WLAN modeling, multi-hop CSMA throughput and fairness analysis, stochastic-geometry modeling, carrier-sense-threshold optimization, vehicular spatial-capacity estimation, and IEEE 802.11ax spatial reuse. However, they leave a gap for a model that is simultaneously: (i) cumulative-sensing-aware, (ii) deterministic and fixed-point-based, (iii) explicitly tied to a finite two-dimensional geometry, and (iv) targeted directly at the mean number of simultaneous transmitters. The present paper addresses this gap by replacing pairwise carrier-sense abstraction with aggregate sensed-energy feasibility and by solving the resulting finite-state admission process through a cumulative-sensing-aware fixed-point formulation.

3 System Model

We consider a two-dimensional CSMA/CA ad-hoc wireless network deployed over a rectangular area

$$\Omega = [0, W] \times [0, H], \tag{1}$$

where W and H denote the width and height of the network region, respectively. The goal is to estimate the spatial-reuse factor of the network, defined as the expected

number of transmitters that can be simultaneously active under the carrier-sensing constraint.

3.1 Candidate Transmitter Set

The continuous deployment area is discretized into a finite set of candidate transmitter locations. Specifically, the area is divided into an $n_x \times n_y$ regular grid. The total number of candidate locations is

$$N = n_x n_y. \tag{2}$$

Each candidate transmitter is placed at the center of one grid cell. Let

$$\mathcal{P} = \{p_1, p_2, \ldots, p_N\} \tag{3}$$

denote the set of all candidate transmitter positions, where $p_i = (x_i, y_i)$ is the coordinate of candidate i. For the grid cell indexed by (u, v), with $u = 0, \ldots, n_x - 1$ and $v = 0, \ldots, n_y - 1$, the corresponding candidate position is

$$p_{u,v} = \left(\left(u + \frac{1}{2} \right) \frac{W}{n_x}, \left(v + \frac{1}{2} \right) \frac{H}{n_y} \right). \tag{4}$$

This grid-center discretization allows the two-dimensional spatial-reuse problem to be represented as a finite-state problem over subsets of $\mathcal{P}$.

3.2 Propagation and Received Sensing Energy

All transmitters are assumed to use the same transmit power P_t. When the transmit power is given in dBm as P_t^{dBm}, its linear-scale value in watts is

$$P_t = 10^{(P_t^{\mathrm{dBm}} - 30)/10}. \tag{5}$$

Similarly, the carrier-sensing or CCA energy-detection threshold θ^{dBm} is converted to watts as

$$\theta = 10^{(\theta^{\mathrm{dBm}} - 30)/10}. \tag{6}$$

We adopt a capped log-distance propagation model. Let L_0 denote the reference path loss at the reference distance of 1 m. The corresponding linear gain factor is

$$B = 10^{-L_0/10}. \tag{7}$$

For two candidate locations p_i and p_j, let

$$d_{ij} = \|p_i - p_j\|_2 \tag{8}$$

be their Euclidean distance. The received sensing energy at candidate i caused by an active transmitter j is modeled as

$$g_{j,i} = P_t \min\left(B, \frac{B}{d_{ij}^{\alpha}} \right), \tag{9}$$

where α is the path-loss exponent. The capping by B avoids unrealistically large received energy at distances smaller than the reference distance.

Let $S \subseteq \mathcal{P}$ denote the set of currently active transmitters. The cumulative sensing energy observed at candidate location i is then

$$E_i(S) = \sum_{p_j \in S} g_{j,i}. \tag{10}$$

This cumulative formulation is important because a candidate transmitter may be blocked not only by a single nearby transmitter, but also by the aggregate received energy generated by multiple active transmitters.

3.3 Carrier-Sensing Feasibility

A candidate transmitter i is feasible in state S if it is not already active and if the cumulative sensing energy at its location does not exceed the CCA threshold. Therefore, the feasible candidate set is defined as

$$\mathcal{A}(S) = \{i \in \{1, \ldots, N\} : p_i \notin S,\, E_i(S) \leq \theta\}. \tag{11}$$

If $\mathcal{A}(S) = \emptyset$, no additional transmitter can be admitted under the cumulative carrier-sensing constraint, and the current state is absorbing.

The spatial-reuse factor estimation problem can therefore be stated as follows: starting from the empty active set $S = \emptyset$, estimate the expected number of transmitters that can be sequentially admitted before the feasible set becomes empty.

4 Cumulative-Sensing-Aware Fixed-Point Formulation

4.1 State Representation

The state of the system is represented by the active transmitter set

$$S \subseteq \mathcal{P}. \tag{12}$$

Since there are N candidate locations, the total number of possible states is

$$|\mathcal{S}| = 2^N. \tag{13}$$

Each state can be encoded by a binary mask of length N, where bit i indicates whether candidate transmitter i is currently active.

For a given state S, define $V(S)$ as the expected number of additional transmitters that can still be admitted from state S until the carrier-sensing process terminates. The desired spatial-reuse estimate is then

$$m(W, H) = V(\emptyset). \tag{14}$$

4.2 Fixed-Point Equation

If there is no feasible candidate in state S, the process terminates and no further transmitter can be added. Thus,

$$V(S) = 0, \quad \text{if } \mathcal{A}(S) = \emptyset. \tag{15}$$

Otherwise, one feasible candidate is selected as the next active transmitter. We assume that all feasible candidates have equal probability of being selected. This assumption approximates the symmetric contention behavior of CSMA/CA, where feasible nodes compete for channel access and one of them wins the next transmission opportunity.

Therefore, for $\mathcal{A}(S) \neq \emptyset$, the value function satisfies

$$V(S) = 1 + \frac{1}{|\mathcal{A}(S)|} \sum_{i \in \mathcal{A}(S)} V(S \cup \{p_i\}). \tag{16}$$

The first term accounts for the newly admitted transmitter, while the second term is the expected number of additional transmitters that can still be admitted after adding candidate i to the active set.

Equation (16) is the central fixed-point equation of the proposed method. Unlike pairwise exclusion models, the feasible set $\mathcal{A}(S)$ is computed using the cumulative sensing energy in (10). As a result, the model explicitly captures the aggregate carrier-sensing effect produced by multiple simultaneous transmitters.

4.3 Matrix Precomputation

To efficiently evaluate the cumulative sensing condition, we first precompute the pairwise gain matrix

$$\mathbf{G} = [g_{j,i}]_{N \times N}, \tag{17}$$

where $g_{j,i}$ is given by (9). Then, for every state S, the cumulative sensing energy vector is computed as

$$\mathbf{E}(S) = [E_1(S), E_2(S), \ldots, E_N(S)]\,. \tag{18}$$

Using the binary-mask representation, these cumulative energy vectors can be recursively precomputed. If S is a nonempty state and j is one active transmitter in S, then

$$\mathbf{E}(S) = \mathbf{E}(S \setminus \{p_j\}) + \mathbf{G}_{j,:}, \tag{19}$$

where $\mathbf{G}_{j,:}$ is the row of the gain matrix corresponding to transmitter j. This precomputation avoids recomputing the cumulative energy from scratch for every state and every candidate.

4.4 Fixed-Point Iteration Algorithm

The fixed-point equation is solved by iterative updates over all 2^N states. Let $V^{(k)}(S)$ denote the value estimate at iteration k. Starting from

$$V^{(0)}(S) = 0, \quad \forall S \subseteq \mathcal{P}, \tag{20}$$

Algorithm 1 Cumulative-Sensing-Aware Fixed-Point Iteration

Require: Area size W, H; grid size n_x, n_y; transmit power P_t; reference gain B; path-loss exponent α; CCA threshold θ; tolerance ε

Ensure: Estimated spatial-reuse factor $m(W, H)$

Generate candidate set $\mathcal{P} = \{p_1, \ldots, p_N\}$ using grid-center placement
Compute pairwise gain matrix $\mathbf{G}$ using (9)
Precompute cumulative energy vector $\mathbf{E}(S)$ for every state $S \subseteq \mathcal{P}$
Initialize $V^{(0)}(S) \leftarrow 0$ for all $S \subseteq \mathcal{P}$
$k \leftarrow 0$
repeat
    $\Delta \leftarrow 0$
    for all $S \subseteq \mathcal{P}$ **do**
        Compute feasible set $\mathcal{A}(S)$ using (11)
        if $\mathcal{A}(S) = \emptyset$ **then**
            $V^{(k+1)}(S) \leftarrow 0$
        else
            $V^{(k+1)}(S) \leftarrow 1 + \dfrac{1}{|\mathcal{A}(S)|} \displaystyle\sum_{i \in \mathcal{A}(S)} V^{(k)}(S \cup \{p_i\})$
        end if
        $\Delta \leftarrow \max\left(\Delta, |V^{(k+1)}(S) - V^{(k)}(S)|\right)$
    end for
    $k \leftarrow k + 1$
until $\Delta < \varepsilon$
return $m(W, H) = V^{(k)}(\emptyset)$

the update rule is

$$V^{(k+1)}(S) = \begin{cases} 0, & \mathcal{A}(S) = \emptyset, \\ 1 + \dfrac{1}{|\mathcal{A}(S)|} \displaystyle\sum_{i \in \mathcal{A}(S)} V^{(k)}(S \cup \{p_i\}), & \mathcal{A}(S) \neq \emptyset. \end{cases} \tag{21}$$

The iteration stops when the maximum difference between two consecutive value functions is smaller than a tolerance ε:

$$\max_{S \subseteq \mathcal{P}} \left| V^{(k+1)}(S) - V^{(k)}(S) \right| < \varepsilon. \tag{22}$$

The complete procedure is summarized in Algorithm 1.

4.5 Existence and Uniqueness

The fixed-point equation has a unique finite solution. This follows from the structure of the state transition. From any nonterminal state S, the next state is always of the form $S \cup \{p_i\}$, where $i \in \mathcal{A}(S)$. Therefore, every transition strictly increases the

number of active transmitters:

$$|S \cup \{p_i\}| = |S| + 1. \tag{23}$$

Consequently, the state-transition graph is acyclic and the process must terminate after at most N admissions. Terminal states with $\mathcal{A}(S) = \emptyset$ have value zero, and the values of all other states are uniquely determined by backward recursion from larger active sets to smaller active sets.

Although a direct backward dynamic-programming solution is possible, the fixed-point iteration in (21) provides a simple and implementation-friendly method. Since the dependency of $V(S)$ is only on states with larger cardinality, the iterative update propagates terminal-state information toward the empty state. In exact arithmetic, convergence occurs after a finite number of sweeps bounded by the maximum possible number of admitted transmitters.

4.6 Computational Complexity

The exact formulation requires enumerating all subsets of the N candidate locations. Therefore, the number of states is 2^N. The pairwise gain matrix requires

$$O(N^2) \tag{24}$$

operations and storage. Precomputing the cumulative energy vector for all states requires

$$O(N2^N) \tag{25}$$

storage and computational cost. Each fixed-point sweep evaluates the feasible set for all states, leading to a per-iteration cost of

$$O(N2^N). \tag{26}$$

Since the maximum admission length is at most N, the overall exact solution has exponential complexity in N. Thus, the proposed method is best viewed as an exact finite-state estimator for moderate-size candidate sets and as a benchmark for validating scalable approximations in larger networks.

4.7 Interpretation of the Estimate

The final value

$$m(W, H) = V(\emptyset) \tag{27}$$

represents the expected number of simultaneous transmitters admitted by the cumulative carrier-sensing process over the two-dimensional region Ω. A larger value of $m(W, H)$ indicates higher spatial reuse. The estimate naturally depends on the area dimensions (W, H), candidate density N, transmit power P_t, CCA threshold θ, and path-loss exponent α. Larger deployment regions and larger path-loss exponents generally increase spatial reuse, while lower CCA thresholds make nodes more sensitive to aggregate energy and therefore reduce the number of simultaneous transmitters.

It is important to distinguish the spatial-reuse metric considered in this paper from conventional throughput capacity. The value $m(W, H)$ is a dimensionless concurrency metric: it estimates the expected number of transmitters that can be active simultaneously under cumulative carrier sensing. If the average time required to transmit one packet is denoted by T_{pkt}, then a corresponding packet-level spatial-reuse capacity can be written as

$$C_{\mathrm{pkt}}(W, H) = \frac{m(W, H)}{T_{\mathrm{pkt}}}, \tag{28}$$

in packets per second. Similarly, if the average packet size is L_{pkt} bits, the corresponding bit-rate capacity can be approximated as

$$C_{\mathrm{bit}}(W, H) = \frac{m(W, H) L_{\mathrm{pkt}}}{T_{\mathrm{pkt}}}. \tag{29}$$

However, the present work focuses on estimating and validating the fundamental spatial-reuse factor $m(W, H)$, since this quantity captures the geometric and carrier-sensing limit on simultaneous CSMA/CA transmissions independently of a particular packet size, modulation rate, or MAC overhead model.

5 ns-3 Validation

This section validates the proposed cumulative-sensing-aware fixed-point formulation against packet-level simulations conducted in ns-3.46.1. The objective is not to reproduce the full IEEE 802.11 MAC dynamics in the analytical model, but rather to verify whether the proposed fixed-point estimator can accurately predict the mean number of simultaneously active transmitters under realistic ad-hoc Wi-Fi contention and carrier-sensing behavior.

5.1 Simulation Setup

The ns-3 validation scenario considers a two-dimensional ad-hoc Wi-Fi network in which stations are statically deployed over a rectangular area of size $W \times H$. Unless otherwise stated, the stations are placed at the centers of a regular 5×4 grid, giving $N = 20$ candidate transmitters. This deployment is consistent with the candidate-location grid used by the fixed-point solver, so that both the analytical estimator and the ns-3 simulation evaluate the same geometric configuration.

The wireless network is configured in ad-hoc mode using `AdhocWifiMac`. Each station generates saturated-like UDP broadcast traffic toward `255.255.255.255`, so that transmissions do not depend on ARP resolution or unicast peer availability. The PHY layer uses a log-distance propagation model with path-loss exponent α. The reference path loss is set to $L_0 = 46.6777$ dB at 1 m, matching the value used in the fixed-point implementation. The default transmit power is $P_t = 16$ dBm, corresponding to 0.039811 W. The carrier-sensing threshold θ is configured through the CCA energy-detection threshold.

The ns-3 script records PHY-layer transmission-start events using the `PhyTxBegin` trace source. For each sampling window $[t, t+\Delta T]$, the simulator counts the number of

Table 1 Main ns-3 simulation parameters.

Parameter	Value
Simulator	ns-3.46.1
Wi-Fi mode	Ad-hoc Wi-Fi
MAC type	`AdhocWifiMac`
Default standard	IEEE 802.11ax
PHY rate control	Constant-rate Wi-Fi manager
Traffic type	UDP broadcast
Broadcast address	`255.255.255.255:9000`
Packet size	1472 bytes
UDP sending rate	100 packets/s/station
Simulation time	20 s
Sampling starts from	$t = 1$ s
Sampling-window length	$\Delta T = 0.00224$ s
Mobility model	Static grid deployment
Default grid	5×4 stations
Default number of stations	$N = 20$
Transmit power	16 dBm
Reference path loss	46.6777 dB at 1 m
Propagation model	Log-distance path loss
Default path-loss exponent	$\alpha = 3.0$
Default CCA threshold	-62 dBm
Reported metric	Mean simultaneous transmitters
Uncertainty measure	95% confidence interval

Table 2 Validation scenarios.

Scenario	Varied parameter	Fixed parameters
Area-size variation	$W = H$ from 8 m to 100 m	$N = 20$, $\alpha = 3$, $\theta = -62$ dBm
Node-count variation	N from 1 to 20	$W = H = 30$ m, $\alpha = 3$, $\theta = -62$ dBm
Path-loss variation	$\alpha \in \{2, 2.5, 3, 3.5, 4\}$	$N = 20$, $\theta = -62$ dBm
CCA-threshold variation	$\theta \in \{-62, -72, -82\}$ dBm	$N = 20$, $\alpha = 3$

unique stations that start at least one PHY transmission. A post-processing collision filter is then applied: if two transmitters in the same sampling window are separated by less than the CCA-distance threshold $D_{\max}$, the later transmitter is removed from the simultaneous-transmitter count. This gives a packet-level reference value for the mean number of simultaneous transmitters.

The main simulation parameters are summarized in Table 1.

For each scenario, the fixed-point estimator is executed using the same geometry, transmit power, reference loss, path-loss exponent, and CCA threshold as the ns-3 simulation. The fixed-point result is denoted by $m(W, H)$, while the ns-3 reference is reported as the sample mean of the simultaneous-transmitter count with a 95% confidence interval.

5.2 Validation Scenarios

Four groups of experiments are considered, as summarized in Table 2. These experiments are designed to stress the model under changes in deployment area, node density, propagation attenuation, and carrier-sensing sensitivity.

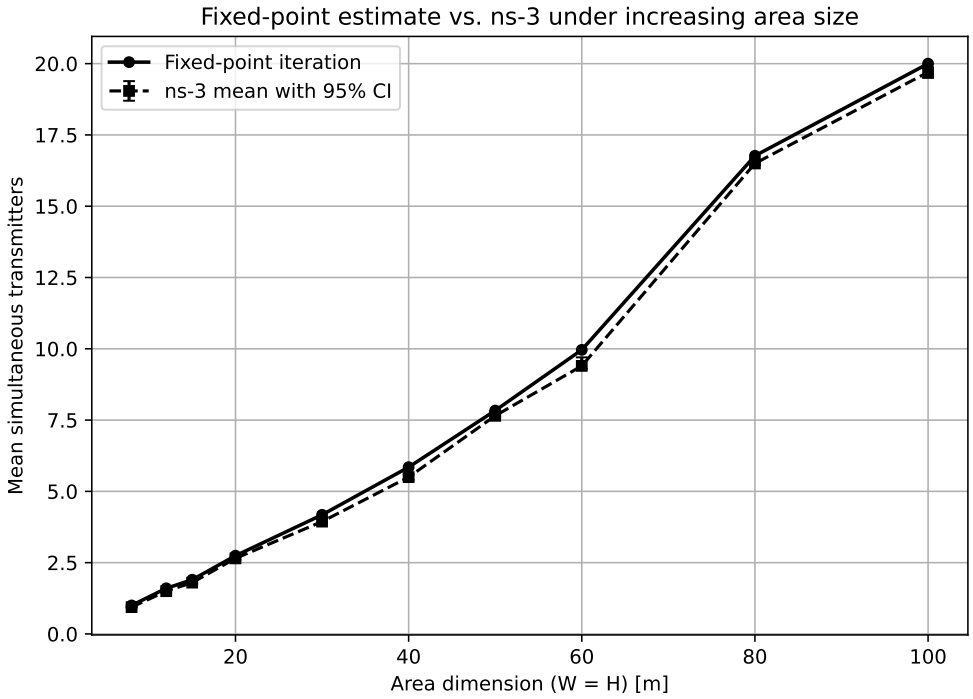


Fig. 1 Fixed-point estimate and ns-3 validation under increasing area size, with $N = 20$, $\alpha = 3$, and $\theta = -62$ dBm.

5.3 Effect of Deployment Area

Figure 1 compares the fixed-point estimate and the ns-3 mean when the number of stations is fixed at $N = 20$ and the deployment area increases from 8×8 m to 100×100 m. The path-loss exponent is fixed at $\alpha = 3$, and the CCA threshold is fixed at -62 dBm.

The result shows a clear monotonic increase in the number of simultaneous transmitters as the deployment area becomes larger. This behavior is expected: as the distance between grid-center stations increases, the received carrier-sensing energy from active transmitters decreases, and more candidates become feasible under the CCA constraint. At small area sizes, such as 8×8 m, the network is strongly carrier-sensing limited and only about one transmitter can be active. As the area grows, spatial reuse gradually improves. At 100×100 m, the fixed-point estimate reaches the maximum possible value of 20 active transmitters, while ns-3 reports a value slightly below 20.

The fixed-point curve closely follows the ns-3 curve over the whole range. A small positive bias is visible, especially in the middle and large-area regimes. This is reasonable because the fixed-point formulation represents an idealized sequential admission

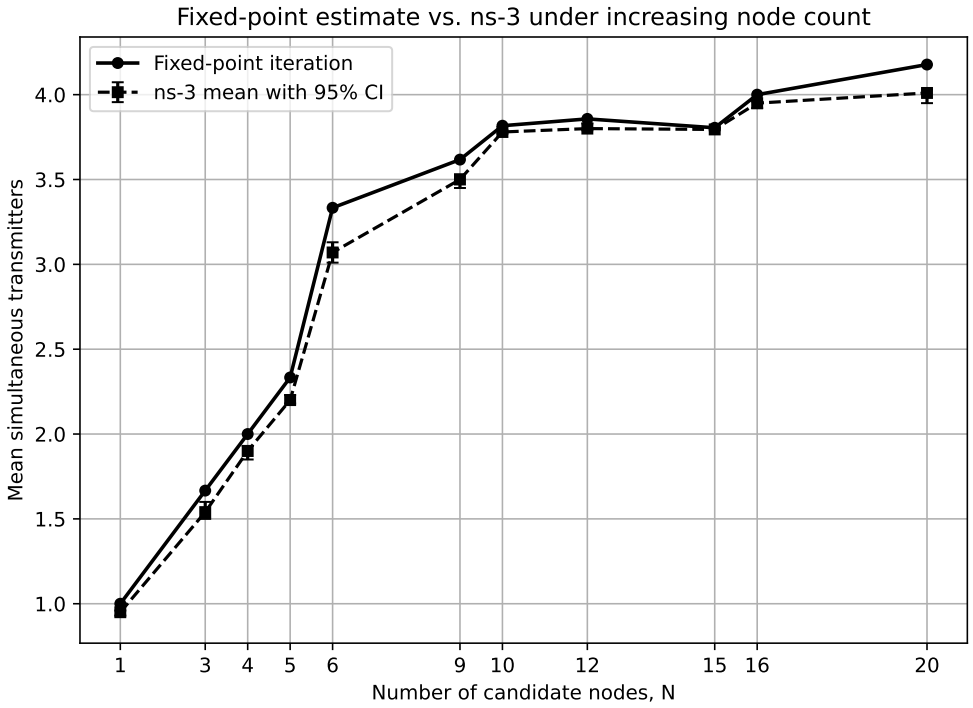


Fig. 2 Fixed-point estimate and ns-3 validation under increasing number of candidate nodes, with $W = H = 30$ m, $\alpha = 3$, and $\theta = -62$ dBm.

process governed by cumulative sensing, whereas ns-3 includes packet timing, contention, random backoff, PHY transmission events, and the collision-filtering procedure. Nevertheless, the trend and magnitude are accurately reproduced, confirming that the proposed formulation captures the dominant spatial-reuse mechanism.

5.4 Effect of Candidate-Set Density and Grid Geometry

Figure 2 evaluates the effect of increasing the number of candidate stations while keeping the area fixed at 30×30 m. The path-loss exponent and CCA threshold are kept at $\alpha = 3$ and $\theta = -62$ dBm, respectively.

Unlike the area-size experiment, increasing the number of candidate nodes does not lead to a linear increase in the number of simultaneous transmitters. Instead, the spatial-reuse level increases rapidly at first and then saturates around four simultaneous transmitters. This confirms that the limiting factor is not simply the number of available nodes, but the number of nodes that can be packed into the fixed area while satisfying the cumulative carrier-sensing constraint.

The slight non-monotonic behavior around some grid sizes is also meaningful. Because different values of N correspond to different grid shapes, the candidate sets are not strictly nested. For example, a 5×2 grid and a 3×3 grid may

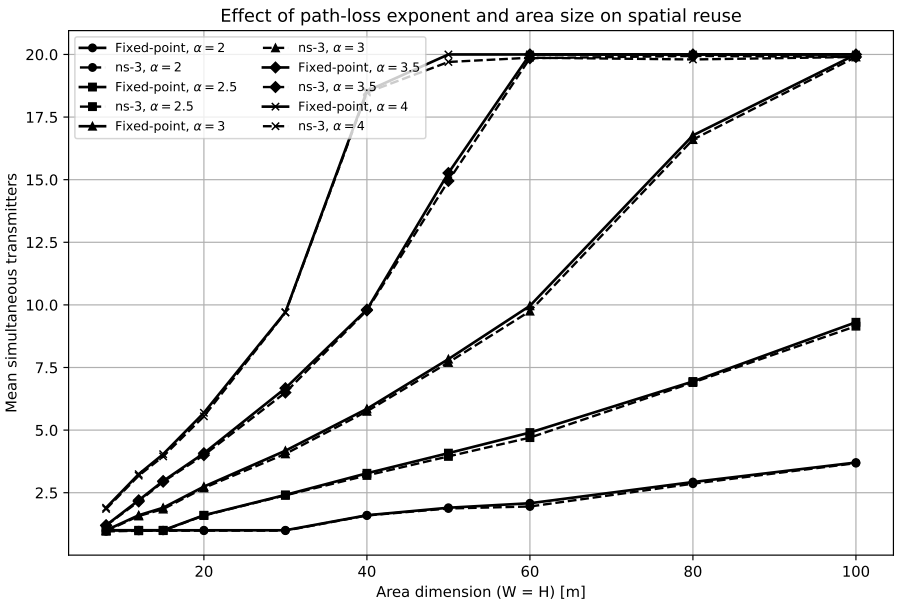


Fig. 3 Effect of path-loss exponent α and area size on the mean number of simultaneous transmitters. Solid lines represent fixed-point estimates, while dashed lines represent ns-3 means. Different markers indicate different values of α.

have different geometric separations even if their numbers of nodes are comparable. Therefore, the simultaneous-transmitter count depends not only on N, but also on the spatial arrangement of the candidates. The fixed-point estimator captures this geometry-dependent behavior and remains close to the ns-3 reference values.

This experiment supports an important interpretation of the proposed method: the estimated value $m(W, H)$ is a spatial-reuse factor under a given finite geometry, not merely a function of node count. Adding more nodes improves the opportunity to find mutually compatible transmitters, but once the area becomes carrier-sensing saturated, additional nodes mainly increase contention rather than usable concurrency.

5.5 Effect of Path-Loss Exponent

Figure 3 shows the impact of the path-loss exponent α on spatial reuse. The number of stations is fixed at $N = 20$, the CCA threshold is fixed at -62 dBm, and the area dimension $W = H$ is varied.

The results show that the path-loss exponent has a strong impact on spatial reuse. For $\alpha = 2$, the received energy decays slowly with distance. Consequently, carrier-sensing regions remain large, and the number of simultaneous transmitters remains small even when the area reaches 100×100 m. In contrast, when $\alpha = 4$, the received energy decays much faster, allowing the network to reach full spatial reuse at a much smaller area size.

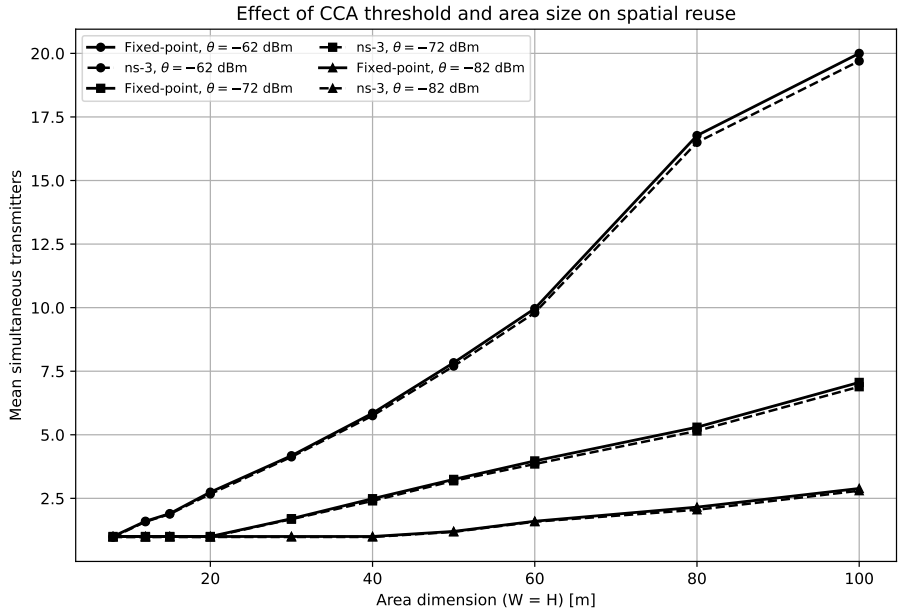


Fig. 4 Effect of CCA threshold θ and area size on the mean number of simultaneous transmitters. Solid lines represent fixed-point estimates, while dashed lines represent ns-3 means. Different markers indicate different CCA thresholds.

The curves can be interpreted as spatial-reuse transition curves. A larger α shifts the transition from low reuse to high reuse toward smaller deployment areas. For example, with $\alpha = 4$, the fixed-point result reaches the maximum of 20 active transmitters by approximately 50×50 m. With $\alpha = 3$, the same full-reuse regime is reached only at a much larger area. This behavior agrees with physical intuition: stronger attenuation reduces the cumulative sensing energy observed by non-active candidates, thereby enlarging the feasible set $\mathcal{A}(S)$ during the sequential admission process.

The agreement between fixed-point and ns-3 is particularly strong in this experiment. The two sets of curves almost overlap for most parameter combinations. This validates the use of the capped log-distance propagation model and confirms that the proposed fixed-point formulation is sensitive to propagation conditions in the same direction and magnitude as packet-level ns-3 simulation.

5.6 Effect of CCA Threshold

Figure 4 evaluates the effect of the CCA energy-detection threshold. The number of stations is fixed at $N = 20$, the path-loss exponent is fixed at $\alpha = 3$, and the area dimension $W = H$ is varied. Three CCA thresholds are considered: -62 dBm, -72 dBm, and -82 dBm.

The CCA threshold controls how sensitive a station is to the energy produced by ongoing transmissions. A higher threshold, such as -62 dBm, makes carrier sensing less conservative and permits more spatial reuse. A lower threshold, such as -82 dBm,

Table 3 Error summary between fixed-point estimates and ns-3 means.

Experiment	Cases	MAE	MAPE
Area-size variation	10	0.226	4.61%
Node-count variation	11	0.101	4.08%
Path-loss variation	50	0.084	1.80%
CCA-threshold variation	30	0.073	2.09%
All scenarios	101	0.097	2.41%

makes stations more sensitive to weak received energy, causing more candidates to be blocked.

The results show this behavior clearly. For $\theta = -62$ dBm, the number of simultaneous transmitters increases rapidly with area size and reaches nearly full reuse at 100×100 m. For $\theta = -72$ dBm, the growth is slower and the number of simultaneous transmitters remains much lower. For $\theta = -82$ dBm, the network remains highly carrier-sensing limited even at large area sizes, reaching fewer than three simultaneous transmitters at 100×100 m.

This experiment is particularly important because it directly validates the cumulative-sensing component of the proposed model. Changing θ changes the feasible set condition

$$E_i(S) \leq \theta, \tag{30}$$

where $E_i(S)$ is the cumulative received energy from all active transmitters. The close match between the fixed-point and ns-3 curves indicates that the proposed formulation captures the threshold-dependent spatial-reuse behavior of CSMA/CA networks.

5.7 Error Analysis

To quantify the agreement between the fixed-point estimator and ns-3, we compute the mean absolute error (MAE) and mean absolute percentage error (MAPE) over each experiment group. Let $\hat{m}_r$ denote the fixed-point estimate and m_r^{ns3} denote the ns-3 mean for case r. The error metrics are defined as

$$\mathrm{MAE} = \frac{1}{R} \sum_{r=1}^{R} \left| \hat{m}_r - m_r^{\mathrm{ns3}} \right|, \tag{31}$$

and

$$\mathrm{MAPE} = \frac{100}{R} \sum_{r=1}^{R} \frac{\left| \hat{m}_r - m_r^{\mathrm{ns3}} \right|}{m_r^{\mathrm{ns3}}}. \tag{32}$$

The numerical error summary is reported in Table 3.

Across all 101 validation cases, the fixed-point estimator achieves an overall MAE of approximately 0.097 simultaneous transmitters and an average relative error of about 2.41%. The error is consistently small across all four validation dimensions. The largest average error occurs in the area-size experiment, where the fixed-point model slightly overestimates ns-3 in the medium-to-large area regime. The path-loss

and CCA-threshold experiments show even smaller average errors, indicating that the model accurately tracks the physical parameters that directly control cumulative sensing.

The fixed-point estimator tends to produce a small positive bias. This is expected for several reasons. First, the fixed-point model assumes an ideal sequential admission process in which one feasible transmitter is admitted at a time according to the cumulative sensing constraint. In contrast, ns-3 includes random backoff, packet timing, MAC-layer contention, and PHY-level transmission-start events. Second, the ns-3 measurement procedure counts transmitters in finite sampling windows and applies a collision filter based on the CCA distance. Third, the analytical formulation estimates the expected number of feasible active transmitters under the sensing rule, whereas the ns-3 result reflects the realized packet-level concurrency under a specific traffic and MAC configuration.

Despite these differences, the close agreement across area size, node count, path-loss exponent, and CCA threshold confirms that cumulative carrier sensing is the dominant mechanism governing the number of simultaneous transmitters in the considered 2D CSMA/CA ad-hoc network. The proposed fixed-point method therefore provides an accurate and computationally controlled estimator of spatial-reuse factor for finite two-dimensional deployments.

5.8 Summary of Validation Findings

The ns-3 validation leads to four main observations. First, increasing the deployment area improves spatial reuse because larger inter-node distances reduce cumulative received sensing energy. Second, increasing the number of nodes in a fixed area improves reuse only up to a saturation point, showing that spatial reuse is constrained by geometry and carrier sensing rather than by the number of contenders alone. Third, increasing the path-loss exponent significantly improves spatial reuse because interference and sensing energy decay faster with distance. Fourth, lowering the CCA threshold reduces spatial reuse because nodes become more sensitive to weak aggregate energy.

Overall, the proposed fixed-point formulation reproduces both the qualitative trends and the quantitative values observed in ns-3. This validates the central modeling assumption of the paper: the expected number of simultaneous CSMA/CA transmitters in a two-dimensional finite network can be accurately estimated by a cumulative-sensing-aware fixed-point process.

6 Limitations

Although the proposed fixed-point formulation accurately estimates the spatial-reuse factor in the considered scenarios, several limitations should be acknowledged. First, the exact solver enumerates all active-transmitter subsets and therefore has exponential complexity in the number of candidate locations. As a result, the current implementation is suitable mainly for moderate-size finite grids and should be viewed as an exact reference model rather than a large-scale online algorithm.

Second, the current formulation assumes static grid-based candidate positions and homogeneous transmitters. Real ad-hoc networks may involve random node placement, mobility, heterogeneous transmit powers, traffic asymmetry, and time-varying channel conditions. These factors may change the feasible active-transmitter set and should be incorporated in future extensions.

Third, the admission process is idealized. The model assumes that one feasible transmitter is selected at each step, with equal probability among all feasible candidates. This captures the average effect of symmetric CSMA/CA contention, but it does not explicitly model backoff counters, retransmissions, queue dynamics, capture effects, hidden terminals, or detailed PHY/MAC timing.

Finally, the ns-3 validation metric is an operational packet-level proxy for simultaneous transmissions. It is based on PHY transmission-start events observed in finite sampling windows and a post-processing collision filter. Therefore, the close agreement with ns-3 should be interpreted as evidence that the proposed model captures the dominant cumulative carrier-sensing mechanism, rather than as a complete reproduction of all IEEE 802.11 MAC-layer dynamics.

7 Conclusion

This paper presented a cumulative-sensing-aware fixed-point framework for estimating the spatial-reuse factor in two-dimensional CSMA/CA ad-hoc networks. Instead of treating carrier sensing as a simple pairwise exclusion rule, the proposed formulation models the physical behavior of CSMA/CA more directly: a candidate transmitter is admitted only when the aggregate received energy from all already-active transmitters remains below the CCA threshold. This makes the model sensitive not only to internode distance, but also to the global spatial arrangement of concurrent transmitters.

By discretizing the deployment region into finite candidate locations, the spatial-reuse problem was transformed into a finite-state admission process. Each state represents a set of active transmitters, and the expected number of additional admissible transmitters is obtained through a deterministic fixed-point recursion. The resulting estimator is simple, reproducible, and physically interpretable. It exposes how deployment area, candidate density, path-loss exponent, transmit power, and carrier-sensing threshold jointly determine the number of simultaneous CSMA/CA transmissions.

The proposed method was validated against ns-3.46.1 ad-hoc Wi-Fi simulations under four complementary scenarios: increasing deployment area, increasing number of candidate nodes, varying path-loss exponent, and varying CCA threshold. The results show that the fixed-point estimator closely tracks packet-level ns-3 behavior across all scenarios. It correctly reproduces the growth of spatial reuse with area size, the saturation effect under increasing node density, the strong reuse improvement caused by larger path-loss exponents, and the reuse reduction caused by more sensitive CCA thresholds. Across the validation set, the estimator remains quantitatively close to ns-3, while preserving a compact analytical structure that is much easier to interpret than packet-level simulation alone.

The main insight of this work is that spatial reuse in CSMA/CA networks is governed by cumulative sensing geometry. Simultaneous transmission is not merely a matter of how many nodes exist, nor only how far apart two nodes are. Rather, it emerges from the interaction between all active transmitters, the propagation environment, and the CCA threshold. The fixed-point formulation provides a practical way to capture this interaction and to estimate the resulting spatial-reuse factor.

There are several directions for future work. First, the exact finite-state solver has exponential complexity and is therefore suitable mainly for moderate-size candidate sets. Scalable approximations, pruning strategies, sampling-based solvers, or learning-assisted estimators could extend the method to larger deployments. Second, the present model assumes static grid-based candidate positions; future work may consider random spatial point processes, mobility, and heterogeneous node distributions. Third, the model can be enriched with more detailed PHY/MAC effects, including fading, capture, hidden terminals, traffic heterogeneity, and adaptive contention parameters. Finally, the same cumulative-sensing fixed-point idea may be extended to three-dimensional wireless networks, such as UAV swarms, where spatial reuse depends on volumetric geometry rather than planar geometry.

In summary, this paper shows that a deterministic fixed-point view of cumulative carrier sensing can serve as an accurate bridge between analytical modeling and packet-level simulation. The proposed framework provides not only a numerical estimator of simultaneous transmitters, but also a clear geometric lens through which the spatial-reuse factor of two-dimensional CSMA/CA networks can be understood.

References

[1] Bianchi, G.: Performance analysis of the IEEE 802.11 distributed coordination function. IEEE Journal on Selected Areas in Communications **18**(3), 535–547 (2000) https://doi.org/10.1109/49.840210

[2] Malone, D., Duffy, K.R., Leith, D.J.: Modeling the 802.11 distributed coordination function in nonsaturated heterogeneous conditions. IEEE/ACM Transactions on Networking **15**(1), 159–172 (2007) https://doi.org/10.1109/TNET.2006.890136

[3] Pham, P.P.: Comprehensive analysis of the IEEE 802.11. Mobile Networks and Applications (2005) https://doi.org/10.1007/s11036-005-3363-x

[4] Szczypiorski, K., Lubacz, J.: Saturation throughput analysis of IEEE 802.11g (ERP-OFDM) networks. Telecommunication Systems (2008) https://doi.org/10.1007/s11235-008-9090-4

[5] Martorell, G., Cano, J.-C., Manzoni, P.: Non-saturated IEEE 802.11 networks: A hierarchical 3d markov model. Computer Networks **80**, 197–212 (2015) https://doi.org/10.1016/j.comnet.2015.02.003

[6] Hajlaoui, N., Jabri, I., Ben Jemaa, M.: An accurate two dimensional markov

chain model for IEEE 802.11n DCF. Wireless Networks (2018) https://doi.org/10.1007/s11276-016-1383-z

[7] Kumar, A., Altman, E., Miorandi, D., Goyal, M.: New insights from a fixed point analysis of single cell IEEE 802.11 WLANs. IEEE/ACM Transactions on Networking **15**(3), 588–601 (2007) https://doi.org/10.1109/TNET.2007.893091

[8] Liew, S.C., Kai, C.H., Leung, H.C., Wong, P.: Back-of-the-envelope computation of throughput distributions in CSMA wireless networks. IEEE Transactions on Mobile Computing **9**(9), 1319–1331 (2010) https://doi.org/10.1109/TMC.2010.89

[9] Garetto, M., Salonidis, T., Knightly, E.W.: Modeling per-flow throughput and capturing starvation in CSMA multi-hop wireless networks. IEEE/ACM Transactions on Networking **16**(4), 864–877 (2008) https://doi.org/10.1109/TNET.2007.902687

[10] Durvy, M., Dousse, O., Thiran, P.: Self-organization properties of CSMA/CA systems and their consequences on fairness. IEEE Transactions on Information Theory **55**(3), 931–943 (2009) https://doi.org/10.1109/TIT.2008.2011427

[11] Jiang, L., Walrand, J.: A distributed CSMA algorithm for throughput and utility maximization in wireless networks. IEEE/ACM Transactions on Networking **18**(3), 960–972 (2010) https://doi.org/10.1109/TNET.2009.2035046

[12] Laufer, R., Kleinrock, L.: The capacity of wireless CSMA/CA networks. IEEE/ACM Transactions on Networking **24**(3), 1518–1532 (2016) https://doi.org/10.1109/TNET.2015.2415465

[13] Fu, L., Liew, S.C., Huang, J.: Effective carrier sensing in CSMA networks under cumulative interference. IEEE Transactions on Mobile Computing **12**(4), 748–760 (2013) https://doi.org/10.1109/TMC.2012.45

[14] Chau, C.K., Ho, W.H., Situ, Z., Liew, S.C., Zhang, J.: Effective static and adaptive carrier sensing for dense wireless CSMA networks. IEEE Transactions on Mobile Computing **16**(2), 355–366 (2017) https://doi.org/10.1109/TMC.2016.2557780

[15] Oni, P.B., Blostein, S.D.: PCS threshold selection for spatial reuse in high density CSMA/CA MIMO wireless networks. IEEE Access **7** (2019) https://doi.org/10.1109/ACCESS.2019.2934751

[16] ElSawy, H., Hossain, E.: A modified hard core point process for analysis of random CSMA wireless networks in general fading environments. IEEE Transactions on Communications **61**(4), 1520–1534 (2013) https://doi.org/10.1109/TCOMM.2013.020813.120594

[17] Alfano, G., Garetto, M., Leonardi, E.: New directions into the stochastic geometry analysis of dense CSMA networks. IEEE Transactions on Mobile Computing **13**(2), 324–336 (2014) https://doi.org/10.1109/TMC.2012.248

[18] Sun, Y., Li, R., Jiang, H., Zheng, J., Ni, L.: Modeling and analysis of random dense CSMA networks. EURASIP Journal on Wireless Communications and Networking (2018) https://doi.org/10.1186/s13638-018-1107-4

[19] Ramachandran, I., Das, A.K., Roy, S.: Analysis of the contention access period of IEEE 802.15.4 MAC. ACM Transactions on Sensor Networks **3**(1) (2007) https://doi.org/10.1145/1210669.1210673

[20] Alves, R.C.A., Margi, C.B.: Behavioral model of IEEE 802.15.4 beacon-enabled mode based on colored petri net. ACM Transactions on Modeling and Performance Evaluation of Computing Systems **2**(3) (2017) https://doi.org/10.1145/3115389

[21] Ortín, J., Gállego, J.R., Canales, M.: Modeling the coexistence of LECIM ALOHA PCA and CSMA/CA in unslotted IEEE 802.15.4 networks. IEEE Internet of Things Journal (2025) https://doi.org/10.1109/JIOT.2025.3539786

[22] Ghandour, A.J., Di Felice, M., Artail, H.A., Bononi, L.: Dissemination of safety messages in IEEE 802.11p/WAVE vehicular network: Analytical study and protocol enhancements. Pervasive and Mobile Computing **11**, 3–18 (2014) https://doi.org/10.1016/j.pmcj.2013.03.003

[23] Giang, A.T., Lambert, A., Busson, A., Gruyer, D.: Topology control in VANET and capacity estimation. In: 2013 IEEE Vehicular Networking Conference (VNC), pp. 135–142. IEEE, ??? (2013). https://doi.org/10.1109/VNC.2013.6737600 . https://doi.org/10.1109/VNC.2013.6737600

[24] Giang, A.T., Busson, A., Renzo, M.D.: Modeling and optimization of CSMA/CA in VANET. Annals of Operations Research **239**(2), 553–568 (2016) https://doi.org/10.1007/s10479-014-1610-x

[25] Giang, A.T., Busson, A., Lambert, A., Gruyer, D.: Spatial capacity of IEEE 802.11p-based VANET: Models, simulations, and experimentations. IEEE Transactions on Vehicular Technology **65**(8), 6454–6467 (2016) https://doi.org/10.1109/TVT.2015.2474156

[26] Khorov, E., Kiryanov, A., Lyakhov, A., Bianchi, G.: A tutorial on IEEE 802.11ax high efficiency WLANs. IEEE Communications Surveys & Tutorials **21**(1), 197–216 (2019) https://doi.org/10.1109/COMST.2018.2871099

[27] Wilhelmi, F., Barrachina-Muñoz, S., Cano, C., Selinis, I., Bellalta, B.: Spatial reuse in IEEE 802.11ax WLANs. Computer Communications **170**, 65–83 (2021) https://doi.org/10.1016/j.comcom.2021.01.028

[28] Jr., L.L., Roy, S.: Performance analysis of the IEEE 802.11ax OBSS_PD-based spatial reuse. IEEE/ACM Transactions on Networking **30**(2), 616–628 (2022) https://doi.org/10.1109/TNET.2021.3117816